

Supporting Information

for *Adv. Funct. Mater.*, DOI: 10.1002/adfm.202213183

Large-Area Smooth Conductive Films Enabled by Scalable Slot-Die Coating of $\text{Ti}_3\text{C}_2\text{T}_x$ MXene Aqueous Inks

*Tiezhu Guo, Di Zhou, Min Gao, Shungui Deng,
Mohammad Jafarpour, Jonathan Avaro, Antonia Neels,
Erwin Hack, Jing Wang, Jakob Heier,* and Chuanfang
(John) Zhang**

Supporting Information

Large-area Smooth Conductive Films Enabled by Scalable Slot-Die Coating of $\text{Ti}_3\text{C}_2\text{T}_x$ MXene Aqueous Inks

Tiezhu Guo, Di Zhou, Min Gao, Shungui Deng, Mohammad Jafarpour, Jonathan Avaro, Antonia Neels, Erwin Hack, Jing Wang, Jakob Heier* and Chuanfang (John) Zhang*

T. Guo, Prof. C. (J). Zhang

College of Materials Science & Engineering, Sichuan University, Chengdu, 610065, Sichuan, China

E-Mail: chuanfang.zhang@scu.edu.cn

T. Guo, S. Deng, M. Jafarpour, Dr. J. Heier

Laboratory for Functional Polymers, Empa, Swiss Federal Laboratories for Materials Science and Technology, Überlandstrasse 129, CH-8600, Dübendorf, Switzerland

E-Mail: Jakob.Heier@empa.ch

T. Guo, Prof. D. Zhou

Key Laboratory of Multifunctional Materials and Structures, Ministry of Education, School of Electronic Science and Engineering, Xi'an Jiaotong University, Xi'an 710049, Shaanxi, China

M. Gao, Prof. J. Wang

Institute of Environmental Engineering, ETH Zürich, Zürich 8093, Switzerland

M. Gao, Prof. J. Wang

Laboratory for Advanced Analytical Technologies, Empa, Swiss Federal Laboratories for Materials Science and Technology, Überlandstrasse 129, Dübendorf 8600, Switzerland

S. Deng, M. Jafarpour

Institute of Materials Science and Engineering, Ecole Polytechnique Federale de Lausanne (EPFL), Station 12, CH-1015 Lausanne, Switzerland

Dr. J. Avaro

Center for X-ray Analytics, Empa, Swiss Federal Laboratories for Materials Science and Technology, Lerchenfeldstrasse 5, CH-9014, St. Gallen, Switzerland

Dr. J. Avaro

Biomimetic Membranes and Textile, Empa, Swiss Federal Laboratories for Materials Science and Technology, Lerchenfeldstrasse 5, St. Gallen CH-9014, Switzerland

Prof. A. Neels

Department of Chemistry, University of Fribourg, Chemin du Musée 9, CH-1700, Fribourg, Switzerland

Prof. A. Neels

Center for X-ray Analytics, Empa, Swiss Federal Laboratories for Materials Science and Technology, Überlandstrasse 129, CH-8600, Dübendorf, Switzerland

Dr. E. Hack

Transport at Nanoscale Interfaces, Empa, Swiss Federal Laboratories for Materials Science and Technology, Überlandstrasse 129, CH-8600 Dübendorf, Switzerland



Figure S1. Digital photographs of $\text{Ti}_3\text{C}_2\text{T}_x$ TCEs on PET and PDMS substrates.

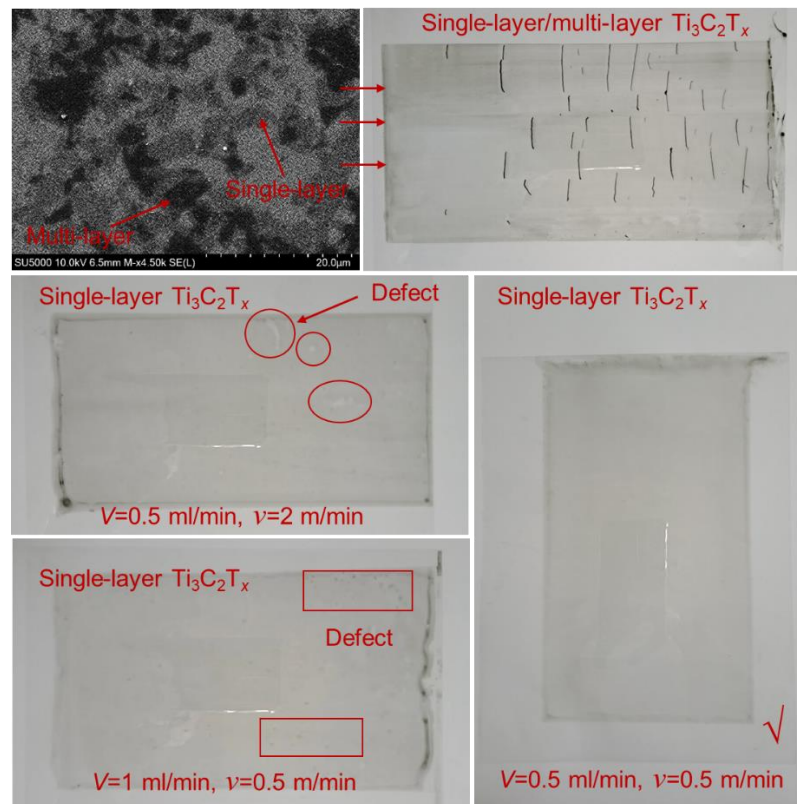
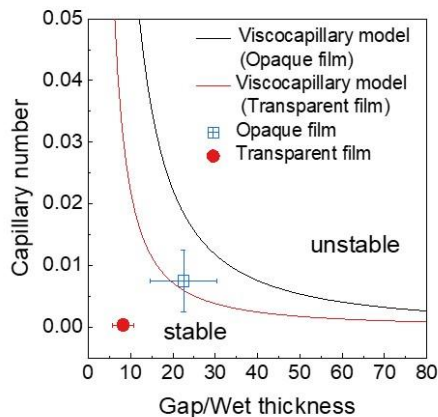


Figure S2. Various factors affecting the uniformity of large area $\text{Ti}_3\text{C}_2\text{T}_x$ TCEs.



	Transparent film	Opaque film
Share rate	218.4 s^{-1}	33.2 s^{-1}
Viscosity	$0.002 \text{ Pa} \cdot \text{s}$	$0.057 \text{ Pa} \cdot \text{s}$
Capillary number	0.00034 ± 0.00016	0.0075 ± 0.005
Gap/Wet thickness	22.6 ± 8	8.2 ± 2.5
$\text{Gap}_{\text{opaque film}} = \sim 250 \mu\text{m}$	Concentration= $20 \sim 25 \text{ mg ml}^{-1}$	
$\text{Gap}_{\text{transparent film}} = \sim 38 \mu\text{m}$	Concentration= $1 \sim 3 \text{ mg ml}^{-1}$	

Figure S3. Stability window for slot die coating (equation 6), and positions of the samples shown in Figure S2.

Relevant for the coating of defect-free wet films is the behavior of the fluid meniscus at the downstream lip of the slot die. Required is a minimum wet film thickness, which can be expressed as a critical capillary number:

$$C_{a, \text{crit}} = n \left(\frac{2}{G-1} \right)^{2/3} \quad (1)$$

whereby $G = \frac{h_{\text{gap}}}{h_{\text{wet}}}$ is the ratio of gap between slot die and substrate and the wet film thickness, $n=0.65$ for viscous films;^[1] while $n=0.21$ for low viscosity inks.^[2] The capillary number is given by

$$C_a = \frac{\mu^* v}{\sigma} \quad (2)$$

with σ , surface tension water. μ , viscosity. v , coating speed. As the inks show shear thinning, we obtain viscosity values from the simplified equation (3):

$$\dot{\gamma} = \frac{v}{h_{\text{gap}}} \quad (3)$$

$\dot{\gamma}$, shear rate (s^{-1}). v , coating speed, h_{gap} , die gap. Here, the die gap of transparent and opaque films are 38 and 250 μm , respectively.

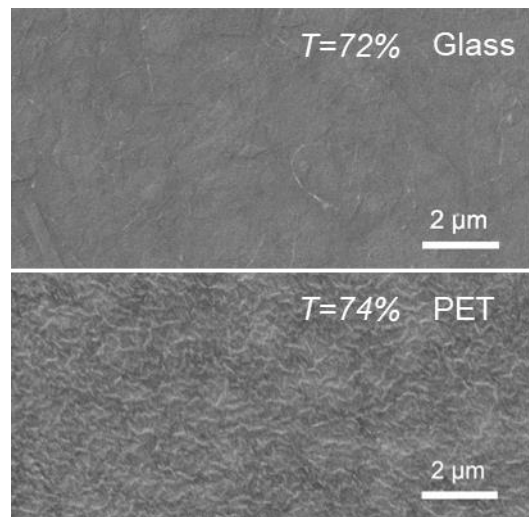


Figure S4. The SEM surface morphology of TCEs on different substrates at a similar transmittance.

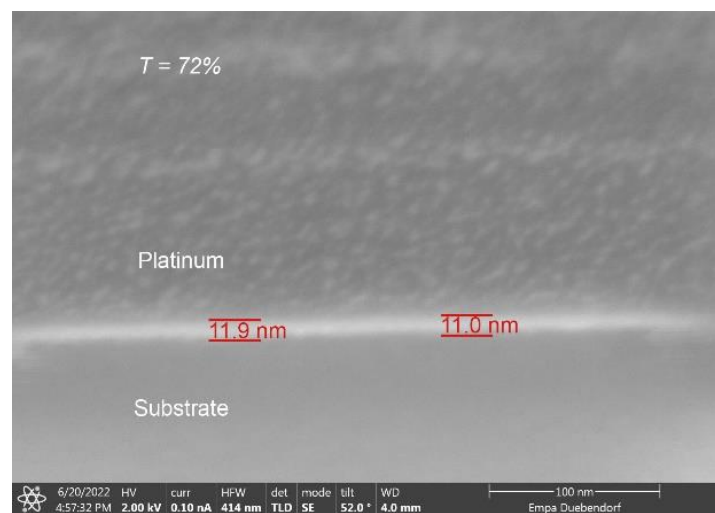


Figure S5. The FIB-SEM cross-sectional image of $T=72\%$ on glass.

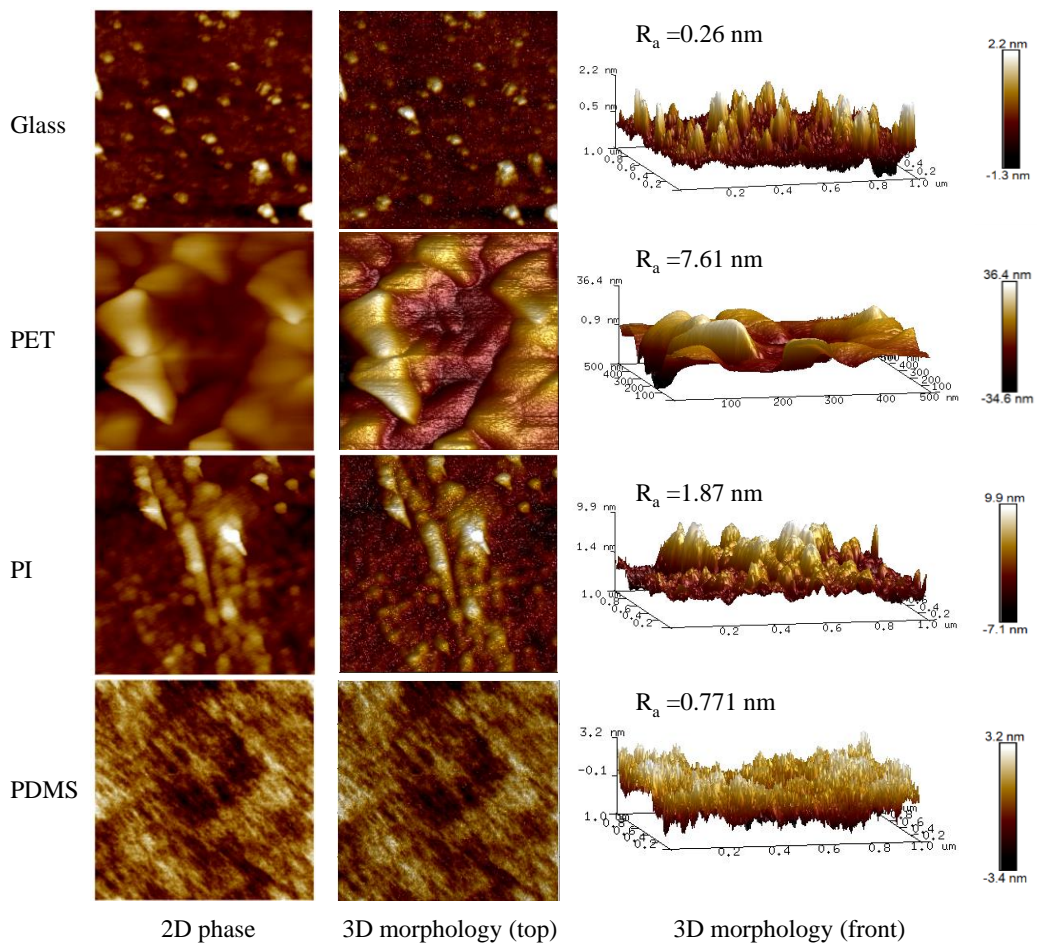


Figure S6. AFM images of surface topography and roughness of different substrates. AFM morphology of different substrates, the image area of glass, PET and PI substrates is $1 \times 1 \mu\text{m}$, and that of PET is $0.5 \times 0.5 \mu\text{m}$.

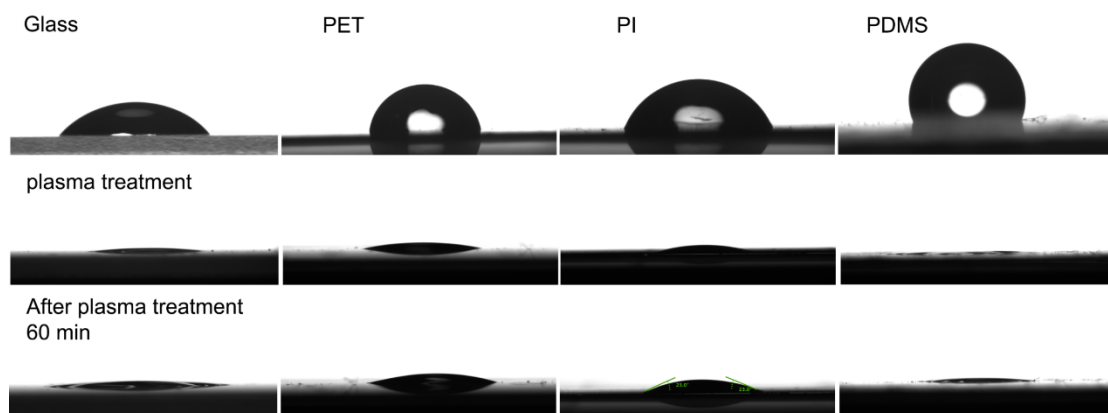


Figure S7. Hydrophilicity of substrate treated with oxygen plasma as a function of time.

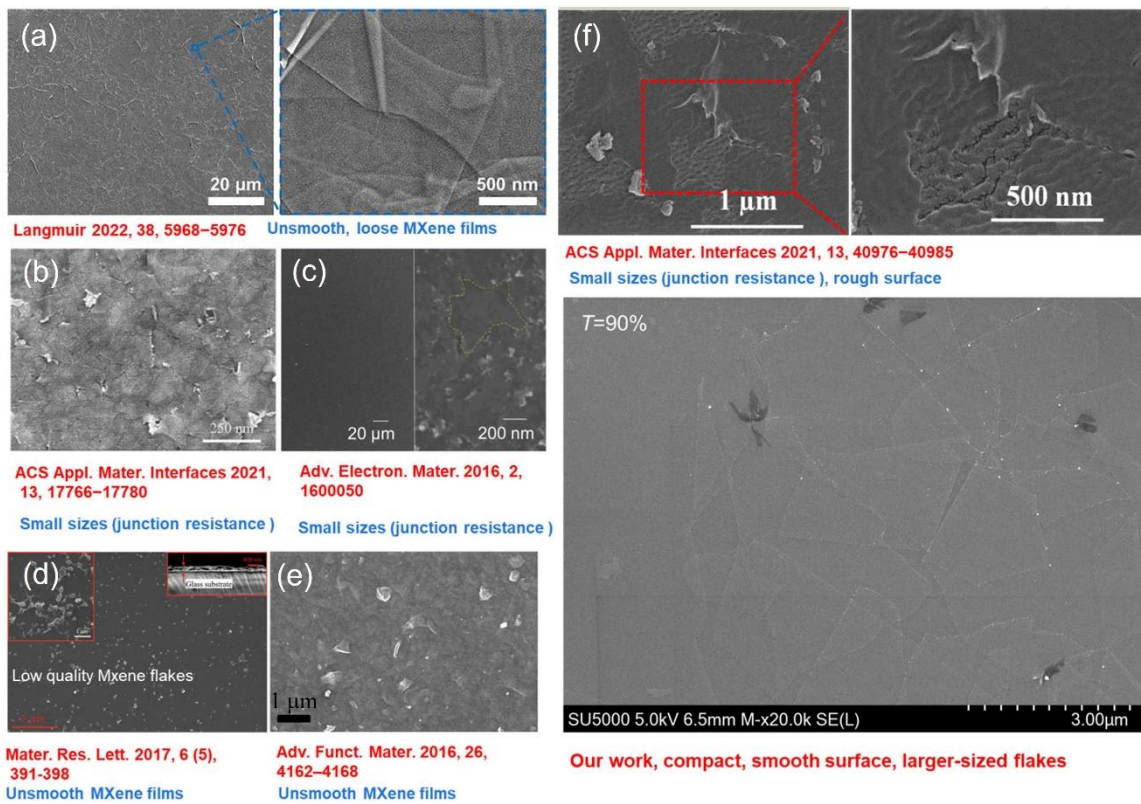


Figure S8. SEM comparison of published work previously with our transparent MXene film.

(a) Reproduced with permission.^[3] Copyright 2022, American Chemical Society. (b) Reproduced with permission.^[4] Copyright 2021, American Chemical Society. (c) Reproduced with permission.^[5] Copyright 2016, John Wiley and Sons. (d) Reproduced with permission.^[6] Copyright 2017, Taylor & Francis Group. (e) Reproduced with permission.^[7] Copyright 2016, John Wiley and Sons. (f) Reproduced with permission.^[8] Copyright 2021, American Chemical Society.

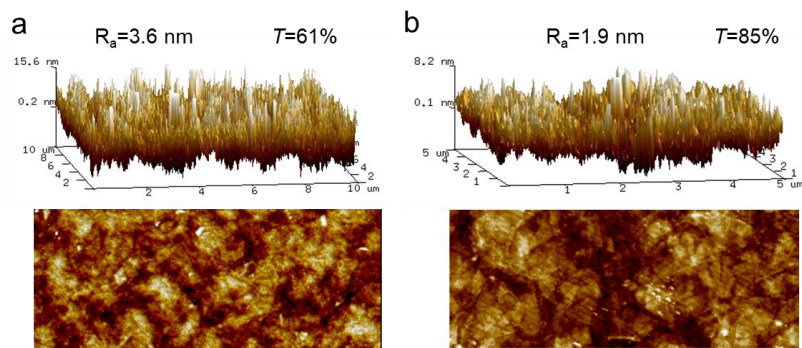


Figure S9. AFM image of $T=61\%$ and $T=85\%$ TCEs.

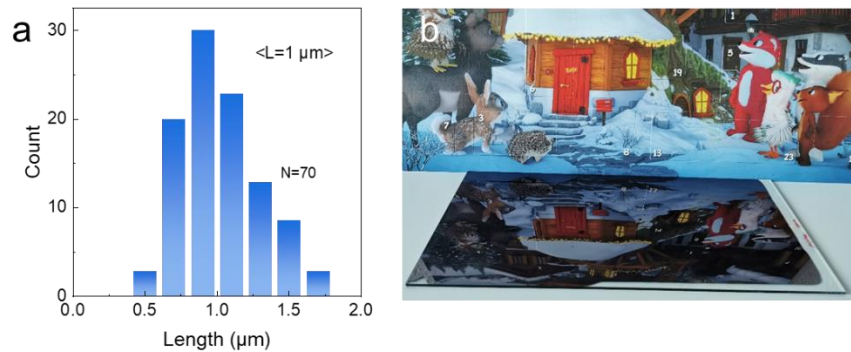


Figure S10. Specular phenomenon of slot-die coated film with small size flakes ($\sim 1 \mu\text{m}$).

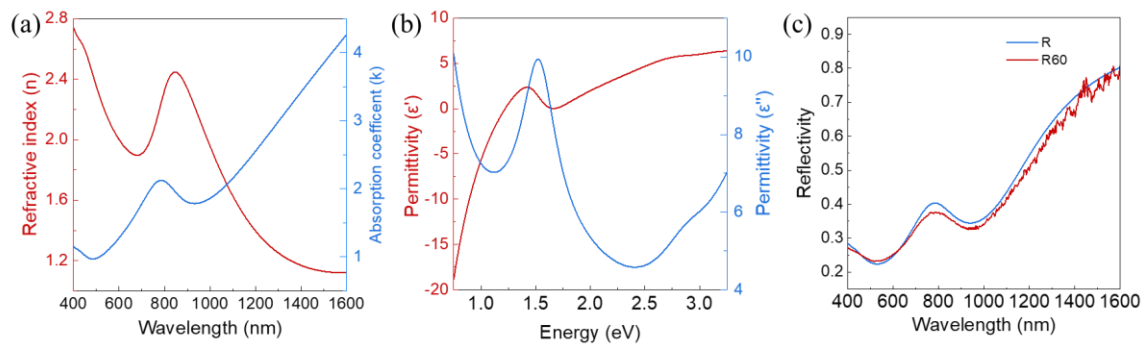


Figure S11. (a) Optical parameters n (refractive index) and k (absorption coefficient) against wavelength. (b) Relative permittivity with real part (ϵ') and imaginary part (ϵ'') against energy. the real and imaginary part of the (relative) permittivity $\epsilon = \epsilon' + i\epsilon''$. (c) Reflection intensity measured from the 200 nm layer at 60° incidence angle (R60) and reflectivity R calculated from the optical parameters for bulk MXene at perpendicular incidence, according to the equation (4)

$$R = \frac{(n-1)^2 + k^2}{(n+1)^2 + k^2} \quad (4)$$

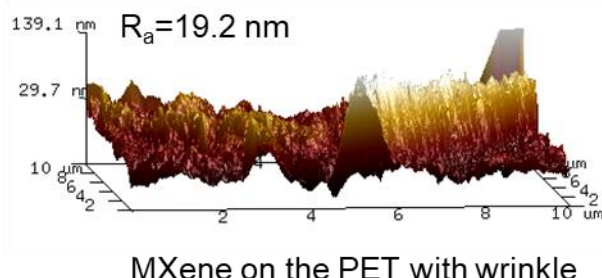


Figure S12. Surface morphology and roughness of $\text{Ti}_3\text{C}_2\text{T}_x$ on PET with wrinkle. The height of wrinkles on PET is about 85 nm, respectively.

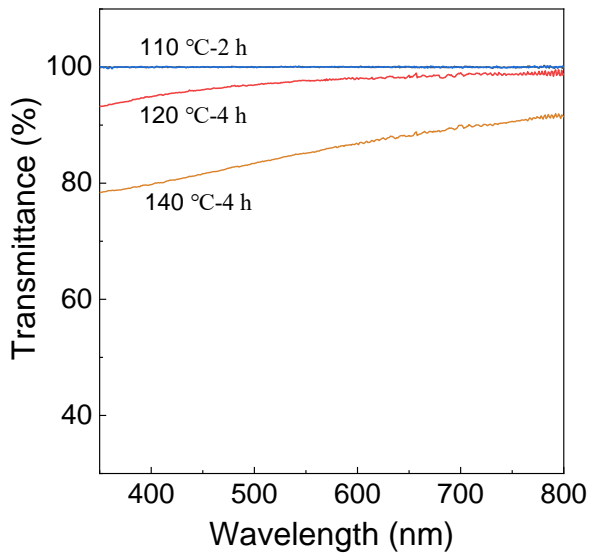


Figure S13. Relationship between heat treatment parameters and transmittance of PET substrate.

The figure shows that the high heat treatment temperature significantly reduces the transmittance of PET, therefore, the transmission spectra were corrected with the transmission spectra of PET annealed at 110 °C.

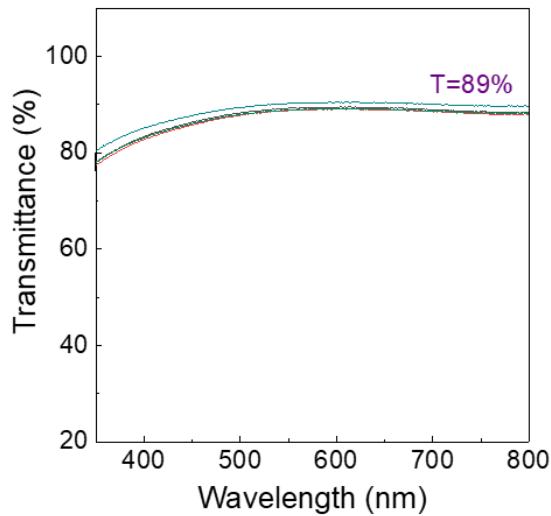


Figure S14. UV-vis spectra of $\text{Ti}_3\text{C}_2\text{T}_x$ TCEs on glass. The transmittance at 550 nm from 5 samples average values, is defined as the transmittance of the film.

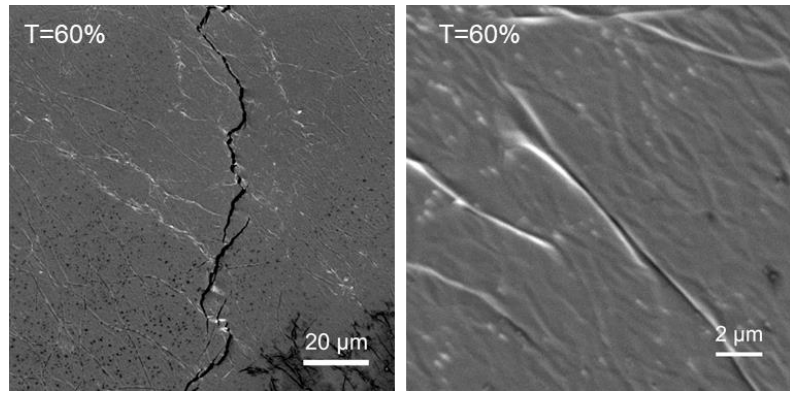


Figure S15. Top-view SEM images of $\text{Ti}_3\text{C}_2\text{T}_x$ on PDMS substrate.

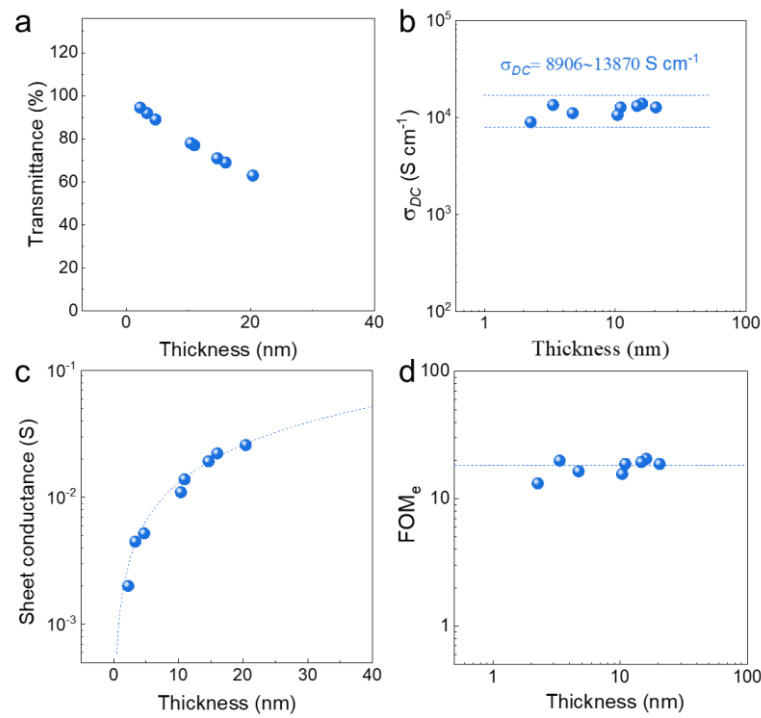


Figure S16. Relationship between $\text{Ti}_3\text{C}_2\text{T}_x$ films thickness and optoelectronic properties. (a) Transmittance, (b) DC conductivity, (c) sheet conductance, (d) Ratio of DC conductivity to optical conductivity.

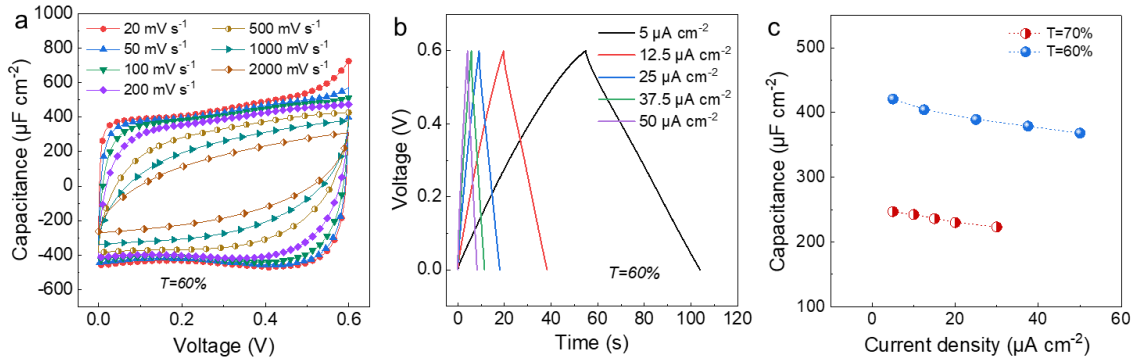


Figure S17. (a) Normalized CV curves at various scan rates of $T=60\%$. (b) GCD curves at different current densities of $T=60\%$. (c) Measured areal capacitance obtained from GCD curves.

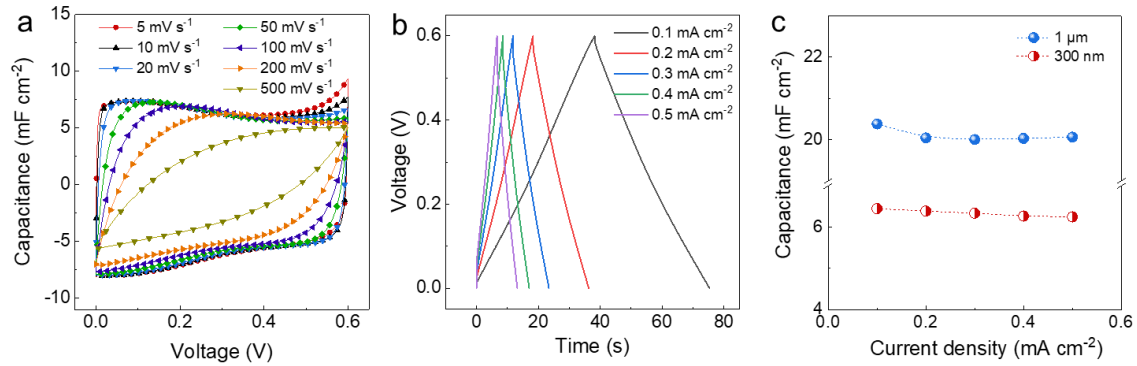


Figure S18. (a) Normalized CV curves at various scan rates of $t=300\text{ nm}$ MSC. (b) GCD curves at different current densities of $t=300\text{ nm}$ MSC. (c) Measured areal capacitance obtained from GCD curves.

Table S1 Conductivity of $\text{Ti}_3\text{C}_2\text{T}_x$ on different substrates

Substrates	Before heating (average sheet resistance, $\Omega \text{ sq}^{-1}$)	After heating (average sheet resistance, $\Omega \text{ sq}^{-1}$)	Average thickness (nm)	Before heating (Conductivity, S cm^{-1})	After heating (Conductivity, S cm^{-1})
Glass	4.42	3.26	230	9 837	13 337
PET	3.66	3.27	302	9 047	10 126
PI	3.07	2.32	336	9 694	12 828
PDMS	2.90	2.07	790	4 365	6 115

Note that the heat treatment of $\text{Ti}_3\text{C}_2\text{T}_x$ films is carried out at 110 °C for 2 h for PET and PDMS substrates to ensure a tolerable temperature range for substrates. The PI and glass substrates are executed at 180 °C for 4 h

Table S2 R_s of TCEs films at various transmittance on different substrates, and data from other literatures.

Samples	Sizes	Manufacturing technique	Transmittance ($T_{550 \text{ nm}}$, %)	Sheet resistance ($\Omega \text{ sq}^{-1}$)	FoM _e	Ref.
$\text{Ti}_3\text{C}_2\text{T}_x$	100~300 nm	Inkjet-printing	24	1 500	0.12	[4]
$\text{Ti}_3\text{C}_2\text{T}_x$	~500 nm	Spray-coating	~51 ~81	~625 ~8 160	0.51	[5]
$\text{Ti}_3\text{C}_2\text{T}_x$	~80 nm	Spin-coating	72 83 90 94	2 010 3 850 11 870 23 660	2	[9]
$\text{Ti}_3\text{C}_2\text{T}_x$	~110 nm	Spin-coating	~72 ~87	~440 ~8 900	3.1	[10]
Ti_2CT_x	~1 μm	Spin-coating	65 80 86 96	128 507 1 100 6 440	5	[6]
V_2CT_x	0.5~1 μm	Spin-coating	~50	~67	6.5	[11]
$\text{Ti}_3\text{C}_2\text{T}_x$	—	Spin-coating	86	330	7.3	[7]
$\text{Ti}_3\text{C}_2\text{T}_x$	~0.5 μm	Dip-coating	~86	~375	9	[12]
$\text{Ti}_3\text{C}_2\text{T}_x$	~1.4 μm	Dip-coating	~88	~600	14	
$\text{Ti}_3\text{C}_2\text{T}_x$	~1.4 μm / Optimized	Dip-coating	~89 ~92	~320 ~1 870	17	
$\text{Ti}_3\text{C}_2\text{T}_x$	1~2 μm	Dip-coating	51 94	40 4 300	14	[13]
$\text{Ti}_3\text{C}_2\text{T}_x$	~3.2 μm	Spin-coating	86 90 94	200 532 1 031	15	[14]
$\text{Ti}_3\text{C}_2\text{T}_x$	6 μm	Slot-die coating	63	38.7	18.5 (glass)	This work
			69	45		

		71	52		
		77	72		
		78	91		
		89	192		
		92	223		
		94.5	498		
		68	70		
		73	98		
		76	100		
		82	186		
		85	236		
		87	434		
		92.4	1 083		
		65	287	—	
		75	9 600	—	

Table S3 of Figure. 5i

Samples	Average electronic conductivety (S cm^{-1})	Ref.
Reduced graphene oxide	550	[15]
Reduced graphene oxide	1 425	[16]
$\text{Ti}_3\text{C}_2\text{T}_x$	3 092	[10]
Ti_2CT_x	5 250	[6]
$\text{Ti}_3\text{C}_2\text{T}_x$	6 500	[7]
$\text{Ti}_3\text{C}_2\text{T}_x$	7 450	[14]
$\text{Ti}_3\text{C}_2\text{T}_x$	7 530	[12]
$\text{Ti}_3\text{C}_2\text{T}_x$	1 3000	This work

Table S4 of Fig. 6e, i

Samples	Transmittance (T _{550 nm} , %)	Power density (μW cm ⁻²)	Energy density(μWh cm ⁻²)	Ref.
Graphene film	67	70	0.00047	[17]
Ti ₃ C ₂ T _x	88	0.0188	0.00163	[13]
	38	1.3	0.01	
Ti ₃ C ₂ T _x	73	0.077	0.0043	[4]
Ti ₃ C ₂ T _x	60	2.592	0.02135	This work
		6.195	0.02065	
		11.808	0.01968	
		21.870	0.01823	
		45.315	0.01511	
	70	1.524	0.01270	
		3.705	0.01235	
		7.119	0.01187	
		13.158	0.01097	
		28.56	0.00952	
300 nm	300 nm	9.315	0.3105	
		18.69	0.3115	
		37.08	0.309	
		88.8	0.296	
		166.2	0.277	
1 μm	1 μm	29.7	0.99	
		57.6	0.96	
		111.6	0.93	
		258	0.86	
		462	0.77	

References

- [1] M. S. Carvalho, H. S. Kheshgi, *AIChE J.* **2000**, *46*, 1907.
- [2] L. Wengeler, K. Peters, M. Schmitt, T. Wenz, P. Scharfer, W. Schabel, *J. Coat. Technol. Res.* **2013**, *11*, 65.
- [3] L. Huang, Y. Lin, W. Zeng, C. Xu, Z. Chen, Q. Wang, H. Zhou, Q. Yu, B. Zhao, L. Ruan, S. Wang, *Langmuir* **2022**, *38*, 5968.
- [4] D. Wen, X. Wang, L. Liu, C. Hu, C. Sun, Y. Wu, Y. Zhao, J. Zhang, X. Liu, G. Ying, *ACS Appl. Mater. Inter.* **2021**, *13*, 17766.
- [5] K. Hantanasirisakul, M. Q. Zhao, P. Urbankowski, J. Halim, B. Anasori, S. Kota, C. E. Ren, M. W. Barsoum, Y. Gogotsi, *Adv. Electron. Mater.* **2016**, *2*, 1600050.
- [6] G. Ying, A. D. Dillon, A. T. Fafarman, M. W. Barsoum, *Mater. Res. Lett.* **2017**, *5*, 391.
- [7] A. D. Dillon, M. J. Ghidiu, A. L. Krick, J. Griggs, S. J. May, Y. Gogotsi, M. W. Barsoum, A. T. Fafarman, *Adv. Funct. Mater.* **2016**, *26*, 4162.
- [8] S. Kumar, D. Kang, V. H. Nguyen, N. Nasir, H. Hong, M. Kim, D. C. Nguyen, Y. J. Lee, N. Lee, Y. Seo, *ACS Appl. Mater. Inter.* **2021**, *13*, 40976.
- [9] M. Ebrahimi, C. T. Mei, *Ceram. Int.* **2020**, *46*, 28114.
- [10] M. Mariano, O. Mashtalir, F. Q. Antonio, W. H. Ryu, B. Deng, F. Xia, Y. Gogotsi, A. D. Taylor, *Nanoscale* **2016**, *8*, 16371.
- [11] G. Ying, S. Kota, A. D. Dillon, A. T. Fafarman, M. W. Barsoum, *FlatChem* **2018**, *8*, 25.
- [12] P. Salles, D. Pinto, K. Hantanasirisakul, K. Maleski, C. E. Shuck, Y. Gogotsi, *Adv. Funct. Mater.* **2019**, *29*, 1809223.
- [13] P. Salles, E. Quain, N. Kurra, A. Sarycheva, Y. Gogotsi, *Small* **2018**, *14*, e1802864.
- [14] C. J. Zhang, B. Anasori, A. Seral-Ascaso, S. H. Park, N. McEvoy, A. Shmeliov, G. S. Duesberg, J. N. Coleman, Y. Gogotsi, V. Nicolosi, *Adv. Mater.* **2017**, *29*, 1702678.

- [15] X. Wang, L. J. Zhi, K. Mullen, *Nano Lett.* **2008**, *8*, 323.
- [16] Y. Y. Liang, J. Frisch, L. J. Zhi, H. Norouzi-Arasi, X. L. Feng, J. P. Rabe, N. Koch, K. Mullen, *Nanotechnology* **2009**, *20*.
- [17] Y. Gao, Y. S. Zhou, W. Xiong, L. J. Jiang, M. Mahjouri-samani, P. Thirugnanam, X. Huang, M. M. Wang, L. Jiang, Y. F. Lu, *APL Mater.* **2013**, *1*, 012101.